Journal of Medicinal Chemistry

Article

pubs.acs.org/jmc

Discovery and Evaluation of Novel Inhibitors of Mycobacterium Protein Tyrosine Phosphatase B from the 6-Hydroxy-benzofuran-5-carboxylic Acid Scaffold

Yantao He,[†] Jie Xu,[†] Zhi-Hong Yu,[†] Andrea M. Gunawan,[‡] Li Wu,[†,‡] Lina Wang,[†] and Zhong-Yin Zhang*[,†]

[†]Department of Biochemistry and Molecular Biology and [‡]Chemical Genomics Core Facility, Indiana University School of Medicine, 635 Barnhill Drive, Indianapolis, Indiana 46202, United States

ABSTRACT: *Mycobacterium tuberculosis* (*Mtb*) protein tyrosine phosphatase B (mPTPB) is a virulence factor secreted by the pathogen and mediates mycobacterial survival in macrophages by targeting host cell immune responses. Consequently, mPTPB represents an exciting new target to combat tuberculosis (TB) infection. We describe a medicinal chemistry oriented approach that transforms a benzofuran salicylic acid scaffold into a highly potent (IC_{50} = 38 nM) and selective mPTPB inhibitor (>50 fold against a large panel of PTPs). Importantly, the inhibitor is capable of reversing the altered host immune responses induced by the bacterial phosphatase and restoring the macrophage's full capacity to secrete IL-6 and undergo apoptosis in response to interferon-γ stimulation, validating the concept that chemical inhibition of mPTPB may be therapeutically useful for novel TB treatment. The study further demonstrates that bicyclic salicylic acid pharmacophores can be used to deliver PTP inhibitors with high potency, selectivity, and cellular efficacy.

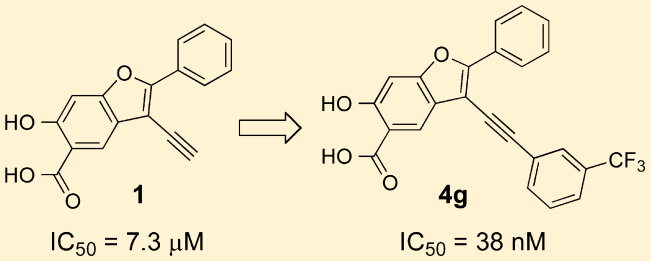

INTRODUCTION

Protein tyrosine phosphorylation-mediated signal transduction is a major post-translational mechanism required for a wide range of cellular functions, including proliferation, differentiation, migration, metabolism, apoptosis, and the immune responses. Perturbation of the delicate balance between the opposing activities of protein tyrosine kinases (PTKs) and protein tyrosine phosphatases (PTPs) causes aberrant tyrosine phosphorylation, which has been implicated in several human diseases including cancer, diabetes/obesity, and autoimmune disorders.[1−3] Hence, PTKs and PTPs are emerging as high-value targets for therapeutic intervention. Notable success has been achieved in targeting signaling pathways regulated by protein tyrosine phosphorylation with more than a dozen of small molecule kinase inhibitors already in the clinic.[4] However, the therapeutic benefits of modulating PTPs are still underexplored due to lack of suitable chemical probes.

Tuberculosis (TB) is the leading cause of worldwide mortality, especially among patients coinfected with HIV and TB. Although several drug regimens are available, current treatments for TB take approximately six to nine months, which makes them difficult for compliance, leading to the appearance of multidrug resistant (MDR) and the virtually untreatable extensively drug-resistant (XDR) TB. Therefore, there is urgent need for new anti-TB agents with novel mechanisms of action to reduce the possibility of a return to an era in which existing drugs are no longer effective.[5,6] TB is a bacterial infection caused by *Mycobacterium tuberculosis* (*Mtb*) that primarily affects the lung. The predominant host cells for *Mtb* are the lung macrophages. Although macrophages play a central role in host defense, recognizing and destroying potential invaders, *Mtb* has evolved several strategies that enable it to survive and replicate within the macrophages.[7] Traditional antibiotics act by inhibiting essential processes in *Mtb* that prevent bacterial growth and replication. This approach results, inevitably, in the selection of mutant strains that developed drug resistance. An emerging and alternative approach is to target pathogen virulence factors to compromise infection process and persistence.[8]

Mtb protein tyrosine phosphatase B (mPTPB) is a virulence factor secreted by *Mtb* into the host macrophage.[9−11] Deletion of mPTPB has no effect on the growth of the pathogen itself but severely attenuates intracellular survival of *Mtb* in infected macrophages and reduces the bacterial load in a guinea pig model of TB infection.[9] These findings suggest that mPTPB may mediate mycobacterial survival in macrophages by targeting host cell processes.[11] Recent studies reveal that mPTPB suppresses the innate immune responses by blocking the extracellular signal-regulated protein kinase (ERK)1/2 and p38 mediated interleukin-6 (IL-6) production and preventing host cell apoptosis by activating the Akt pathway.[12,13]

Given the requirement of mPTPB for host cell survival and the importance of macrophage apoptosis as a defense mechanism to counter *Mtb* infection,[14−18] specific inhibition of mPTPB may augment intrinsic host signaling pathways to

Received: September 11, 2012
Published: January 10, 2013

   dx.doi.org/10.1021/jm301781p | *J. Med. Chem.* 2013, 56, 832−842

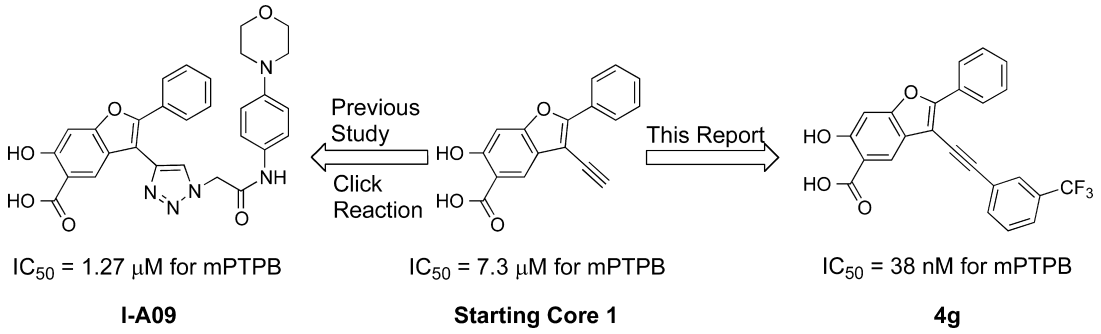

Figure 1. Discovery of mPTPB inhibitors from 6-hydroxybenzofuran-5-carboxylic acid scafford.

eradicate TB infection. Indeed, small molecule inhibitors of mPTPB are capable of reducing intracellular mycobacteria in infected macrophages.[12,13,19] Thus, mPTPB represents an exciting new target for TB with a completely novel mechanism of action. Because mPTPB inhibitors function within the cytosol of macrophages and have no mechanistic overlap with current anti-TB agents, they target the intracellular pool and may compliment/synergize with existing therapeutic approaches to shorten standard TB treatment. Furthermore, since mPTPB acts outside of the bacterium, mPTPB inhibitors need not cross the thick and impenetrable *Mtb* cell wall, which presents a huge barrier to efficient delivery of antibacterial compounds. Understandably, there is intense interest in targeting mPTPB for therapeutic development.[13,19−26] We previously described a benzofuran salicylic acid-based mPTPB inhibitor (I-A09) with highly efficacious cellular activity.[12] However, I-A09 displays a rather modest potency (IC_{50} = 1.26 μM) and selectivity (~10-fold against a panel of mammalian PTPs), which may not be sufficient for therapeutic development. Here we present a medicinal chemistry oriented approach that transforms the benzofuran salicylic acid core into a highly potent and selective mPTPB inhibitor with excellent in vivo efficacy.

RESULTS

Chemistry. The PTP active sites (i.e., pTyr-binding pockets) are highly positively charged, which poses a significant challenge for the development of PTP inhibitors possessing favorable pharmacological properties. Indeed, most current PTP inhibitors are negatively charged and unable to penetrate cell membranes. To address the bioavailability issue, we sought to discover novel nonhydrolyzable pTyr mimetics from natural products because they are evolutionarily selected and validated for interfering and interacting with biological targets in vivo. Benzofuran salicylic acid Core **1** (Figure 1) was found to be an excellent pTyr surrogate for mPTPB with an IC_{50} value of 7.3 μM.[12] Click chemistry was employed to tether Core **1** with 80 azide-containing amines and hydrazines in order to target adjacent secondary binding sites in addition to the active site. This led to the identification of I-A09 (Figure 1), which has an IC_{50} of 1.26 μM for mPTPB and greater than 10-fold preference for mPTPB versus a panel of mammalian PTPs.[12] Despite its highly efficacious cellular activity, the potency and selectivity displayed by I-A09 are relatively modest, and therefore may not be adequate for chemical biological investigation and therapeutic development.

Given the prominent contribution of Core **1** to the binding affinity of I-A09, we sought to improve Core **1**'s potency and selectivity by further modifications on the 3-ethynyl group. To explore the impact of substitutions at the terminal alkynyl group, we initially synthesized compounds **2**, **3**, and **4a** (Table 1), which were prepared via a common key intermediate **11** (Scheme 1) using a previously described method.[12] Commercially available 4-hydroxysalicylic acid reacted with ICl to afford compound **7** in good yield.[27] Upon treatment with acetone and TFAA/TFA, **7** was regioselectively protected to provide dioxanone **8** in modest yield.[28] Dioxanone **8** then reacted with MeI at room temperature in the presence of K_2CO_3/DMSO to give the methylation product **9** with excellent yield. Compound **9** coupled with phenylacetylene in the presence of catalytic amounts of $Pd(PPh_3)_2Cl_2$ and CuI furnished **10**[29,30] which was then subjected to I_2 induced cyclization.[12,31] Cyclization of **10** proceeded exceedingly well and afforded key compound **11** in high yield on a multigram scale (Scheme 1). The iodo-substituted **11** was utilized to prepare compounds **2**, **3**, and **4a** under Sonogashira coupling conditions (Scheme 2).

The ability of compounds **2**, **3**, and **4a** to inhibit the mPTPB-catalyzed hydrolysis of *p*-nitrophenyl phosphate (*p*NPP) was assessed at pH 7 and 25 °C. The IC_{50} values were 5.1, 22, and 0.7 μM, respectively, for compounds **2**, **3**, and **4a** (Table 1). Thus no improvement in potency was observed when ethisterone or methanol was introduced to the terminal alkyne position in Core **1**. In contrast, when a benzene ring was attached to the terminal alkyne position, the resulting compound **4a** experienced a 10-fold increase in binding affinity (IC_{50} = 0.7 μM) relative to the parent Core **1** (IC_{50} = 7.3 μM).

Encouraged by this result, we decided to investigate whether substitutions at the β-benzene ring could further improve the potency and specificity of compound **4a**. A small series of analogues of compound **4a** were prepared via Sonogashira coupling (Scheme 2). Among the various compound **4a** derivatives **4b−i** (Table 1), 3-phenylethynyl-substitued **4b** with a fluorine at the meta position of the β-benzene ring was found to be 4-fold more potent than its parent **4a** for mPTPB. Compound **4c** with a chlorine at the same position showed similar activity as **4b**. Interestingly, substitution at the meta position with a trifluoromethyl group (**4g**) enhanced the binding affinity by more than 18-fold whereas a methoxy substitution (**4d**) at the same position did not exert any significant impact on mPTPB inhibition. Compared to the monosubstituted **4b**, the 3,5-difluorine substituted **4f** had a further 3.3-fold decrease in IC_{50} although the 2.4-difluorine substituted **4e** showed no improvement. Substitution at the para-position by a trifluoromethoxy (**4h**) or a phenoxy (**4i**) group caused a 7.4- and 16.3-fold increase in binding affinity respectively. Finally, the triple bond in compounds **4b**, **4f**, **4g**, **4h**, and **4i** were reduced to a double bond (**5a**,**b**) or a single

dx.doi.org/10.1021/jm301781p | J. Med. Chem. 2013, 56, 832−842

Table 1. IC_{50} (μM) Values of 1, 2, 3, 4a−i, 5a−b, and 6a−d against mPTPB and a Panel of Mammalian PTPs

Cmpd #	Structure	mPTPB	mPTPA	PTP1B	TC-PTP	SHP1	SHP2	LYP	PTP-Meg2	CD45	VHR
1	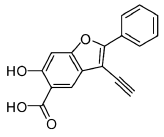	7.3 ± 0.3	63 ± 1	> 50	> 50	> 50	31 ± 0.5	50 ± 5	85 ± 2	80 ± 9	> 50
2	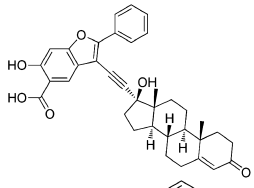	5.09 ± 0.3	>100	> 50	> 50	>100	30 ± 10	12.2 ± 0.5	>100	>100	>100
3	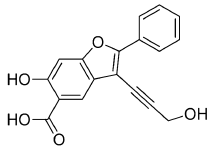	22 ± 4	>100	>100	>100	>100	>100	>100	>100	>100	>100
4a	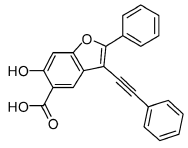	0.7 ± 0.2	7.4 ± 0.5	14.6 ± 0.6	11 ± 1	4.9 ± 0.7	4.0 ± 0.2	4.9 ± 0.3	15.1 ± 0.2	13 ± 1	5.0 ± 2
4b	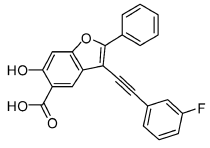	0.18 ± 0.03	5.2 ± 0.3	12 ± 1	20.3 ± 0.7	4.2 ± 0.2	3.6 ± 0.2	3.9 ± 0.2	9.0 ± 0.7	10 ± 1	4.1 ± 0.5
4c	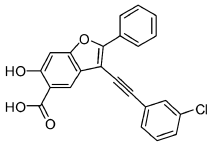	0.13 ± 0.01	1.1 ± 0.1	6.3 ± 0.8	10 ± 1	3.4 ± 0.3	2.3 ± 0.2	0.99 ±0.07	4.0 ± 0.5	9.0 ± 1	16 ± 1
4d	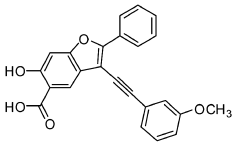	0.54 ± 0.04	34 ± 2	>30	> 30	34 ± 1	38 ± 1	17 ± 1	> 30	>100	> 30
4e	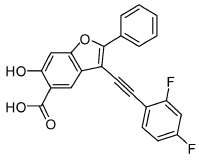	0.26 ± 0.02	4.1 ± 0.3	5.2 ± 0.3	9.0 ± 0.5	2.6 ± 0.3	2.83 ±0.09	3.5 ± 0.2	4.8 ± 0.4	5.5 ± 0.6	3.9 ± 0.8
4f	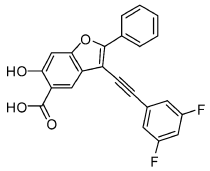	0.054 ±0.004	1.6 ± 0.1	4.5 ± 0.2	6.1 ± 0.5	2.3 ± 0.1	2.2 ± 0.1	1.3 ± 0.1	2.3 ±0.08	4.1 ± 0.5	5.3 ± 0.6
4g	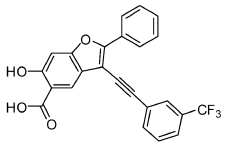	0.038 ±0.002	2.5 ± 0.2	6.7 ± 0.7	13 ± 1	2.3 ± 0.3	1.8 ± 0.2	2.0 ± 0.1	4.3 ± 0.5	4.2 ± 0.5	1.9 ± 0.4
4h	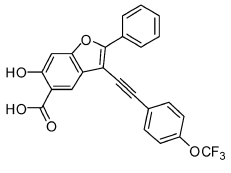	0.095 ± 0.02	2.8 ± 0.3	5.1 ± 0.3	6.7 ± 0.4	2.49 ±0.09	1.8 ± 0.6	2.0 ± 0.1	4.0 ± 0.2	3.6 ± 0.2	2.1 ± 0.2

dx.doi.org/10.1021/jm301781p | J. Med. Chem. 2013, 56, 832−842

Table 1. continued

Cmpd #	Structure	mPTPB	mPTPA	PTP1B	TC-PTP	SHP1	SHP2	LYP	PTP-Meg2	CD45	VHR
4i	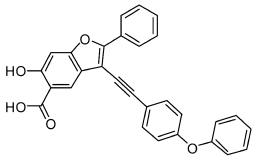	0.043 ±0.003	0.7 ± 0.1	1.2 ± 0.04	1.3 ± 0.2	0.76 ±0.06	0.6 ±0.05	0.63 ±0.03	1.07 ± 0.08	0.9 ±0.04	0.8 ± 0.1
5a	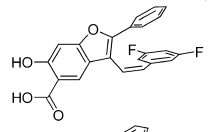	1.2 ± 0.04	6.0 ± 1	8.0 ± 2	9.5 ± 0.8	5.7 ± 0.4	5.0 ± 0.7	3.7 ± 0.5	9.2 ± 0.7	13.1 ±0.07	8.6 ± 0.7
5b	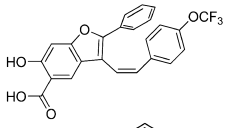	1.2 ± 0.09	6.9 ± 0.7	12 ± 1	9.2 ± 0.6	5.1 ± 0.2	4.5 ± 0.2	4.3 ± 0.3	11.4 ± 0.4	11.6 ± 0.4	5.8 ± 0.4
6a	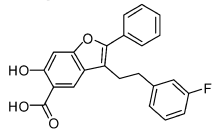	2.0 ± 0.3	29 ± 1	60 ± 20	33 ± 1	11.5 ± 0.3	10.9 ± 0.3	12.4 ± 0.4	110 ± 30	120 ± 80	22 ± 1
6b	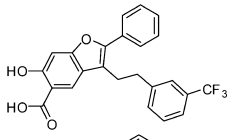	1.03 ± 0.05	5.1 ± 0.4	7.4 ± 0.4	10 ± 0.6	5.3 ± 0.1	4.5 ± 0.2	3.5 ± 0.2	8.6 ± 0.3	10.1 ± 0.4	6.2 ± 0.2
6c	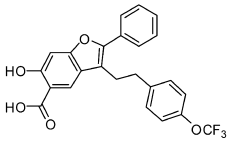	3.4 ± 0.06	5.2 ± 0.3	8.4 ± 0.9	8.9 ± 0.6	7.1 ± 0.2	5.2 ± 0.3	4.1 ± 0.3	8.4 ± 0.2	18.9 ± 0.9	6.7 ± 0.4
6d	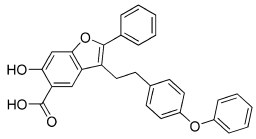	1.1 ± 0.1	3.4 ± 0.3	8.0 ± 1	11.8 ± 0.7	3.7 ± 0.1	3.6 ± 0.2	2.2 ± 0.3	7.7 ± 0.3	14.2 ± 0.9	6.3 ± 0.3

Scheme 1. Synthesis of Key Intermediate 11[a]

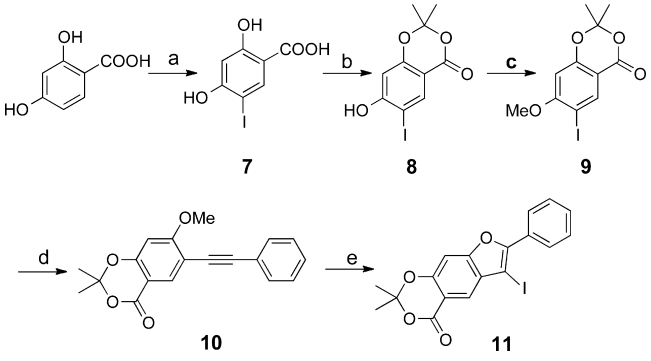

[a]Reagents and conditions: (a) ICl, AcOH, rt; (b) acetone, TFA, TFAA, rt; (c) MeI, K_2CO_3, DMSO, rt; (d) phenylacetylene, $Pd(PPh_3)_2Cl_2$, CuI, DMF, rt; (e) I_2, $NaHCO_3$, MeCN; 70 °C.

bond (**6a–d**) by selective hydrogenation (Scheme 3) in order to evaluate the requirement of the alkyne group. As shown in Table 1, the potency of the triple bond reduced compounds dramatically decreased, indicating that the rigidity and directionality of substitutions at the 3-position of the benzofuran salicylic core are important for optimal interaction with mPTPB.

The results indicated that compound 6-hydroxy-2-phenyl-3-((3-trifluoromethyl)phenyl)benzofuran-5-carboxylic acid (**4g**) was the most potent mPTPB inhibitor in this series with an IC_{50} value of 38 nM (Table 1). Kinetic analysis revealed that compound **4g** is a reversible and noncompetitive inhibitor for mPTPB with a K_i of 44 ± 1.5 nM (Figure 2). To determine the specificity of compound **4g**, its inhibitory activity toward mPTPA and a panel of mammalian PTPs including cytosolic PTPs, PTP1B, TC-PTP, SHP1, SHP2, FAP1, Lyp, PTP-MEG2, and HePTP, the receptor-like PTPs, PTPα, LAR, CD45, and PTPγ, the dual specificity phosphatases VHR, Laforin, VHX, and Cdc14A, and the low molecular weight PTP (LMWPTP) were measured. For comparison, the specificity of compounds **4f** and **4h** were also measured. As shown in Table 2, **4g** is highly selective for mPTPB, exhibiting at least 47-fold selectivity over all other PTPs examined. Together, the results show that **4g** is the most potent and specific mPTPB inhibitors reported to date.

Cellular Activity of Compound 4g. Our ultimate goal is to develop mPTPB-based small molecule therapeutics as new weapons to combat TB infections. Given the excellent potency and selectivity of compound **4g** toward mPTPB, we proceeded to evaluate its ability to inhibit mPTPB activity inside the cell. To define the biochemical mechanism used by mPTPB to evade host immune responses for the benefit of *Mtb* survival in the macrophages, we have established a murine macrophage

dx.doi.org/10.1021/jm301781p | J. Med. Chem. 2013, 56, 832–842

Scheme 2. Synthesis of Compounds 2, 3, and 4a−i[a]

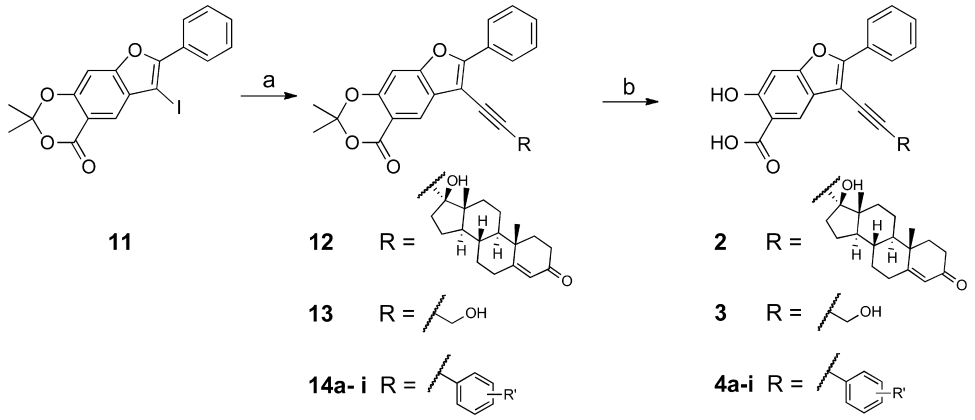

[a]Reagents and conditions: (a) $Pd(PPh_3)_2Cl_2$, CuI, alkyne, DMF, rt; (b) KOH, THF/H_2O, reflux.

Scheme 3. Synthesis of Compounds 5a,b and 6a−d[a]

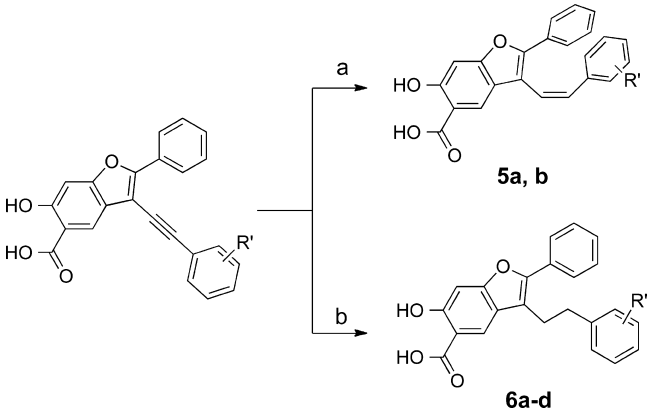

[a]Reagents and conditions: (a) Lindlar catalysis, H_2, THF/MeOH, rt; (b) H_2, Pd/C, THF/MeOH, rt.

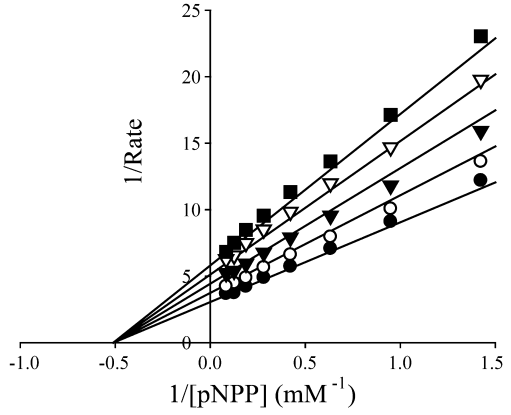

Figure 2. Compound **4g** is a reversible and noncompetitive inhibitor of mPTPB with *p*NPP as a substrate. Line weaver-Burk plot for **4g**-mediated mPTPB inhibition. Compound **4g** concentrations were 0 (●), 10 (○), 20 (▼), 30 (▽), and 40 nM (■), respectively. The K_i value of 44 ± 1.5 nM was determined from three independent measurements.

Raw264.7 cell line ectopically expressing mPTPB.[12] Interferon-γ (IFN-γ), the predominant activator of microbicidal functions of macrophages,[32] is essential for macrophage's antimicrobial activity against diverse intracellular pathogens. We showed that

Table 2. Selectivity of 4g, 4f, and 4h against a Panel of PTPs

PTP	IC_{50} (μM) for **4g**	IC_{50} (μM) for **4f**	IC_{50} (μM) for **4h**
mPTPB	0.038 ± 0.002	0.054 ± 0.004	0.090 ± 0.017
mPTPA	2.5 ± 0.2	1.6 ± 0.1	2.8 ± 0.3
PTP1B	6.7 ± 0.7	4.5 ± 0.2	5.1 ± 0.3
TC-PTP	13 ± 1	6.1 ± 0.5	6.7 ± 0.4
SHP2	1.8 ± 0.2	2.2 ± 0.1	1.8 ± 0.6
SHP1	2.3 ± 0.3	2.3 ± 0.1	2.5 ± 0.1
FAP1	1.3 ± 0.2	1.9 ± 0.04	1.6 ± 0.1
Lyp	2.0 ± 0.1	1.3 ± 0.1	2.0 ± 0.1
PTP-MEG2	4.3 ± 0.5	2.3 ± 0.08	4.0 ± 0.2
HePTP	2.1 ± 0.3	3.3 ± 0.5	1.9 ± 0.3
Laforin	40 ± 10	>30	31 ± 4
VHX	1.4 ± 0.2	2.9 ± 0.3	1.9 ± 0.1
VHR	1.9 ± 0.4	5.3 ± 0.6	2.1 ± 0.2
LMWPTP	4.3 ± 0.6	2.9 ± 0.3	3.0 ± 0.1
Cdc14A	6.0 ± 1.0	21 ± 2	6.0 ± 1.0
PTPα	>10	>10	>10
LAR	>10	>10	>10
CD45	4.2 ± 0.5	4.1 ± 0.5	3.6 ± 0.2
PTPγ	2.6 ± 0.6	5.0 ± 0.3	1.8 ± 0.1

mPTPB inhibits the responses of mPTPB-containing macrophages to IFN-γ by reducing the IFN-γ stimulated IL-6 production through down-regulating the ERK1/2 and p38 pathways. In addition, we also obtained evidence that mPTPB activity is responsible for increased phospho-Akt and decreased apoptosis of macrophages when exposed to IFN-γ. As a result, the Raw264.7 cell line serves as a very convenient model system to evaluate the cellular efficacy of mPTPB inhibitors. We predict that inhibition of mPTPB activity should reverse the effects of mPTPB on ERK1/2, p38, and Akt signaling and restore macrophage's full capacity to secrete IL-6 and undergo apoptosis in response to IFN-γ stimulation.

As shown in Figure 3, Raw264.7 cells expressing mPTPB displayed decreased IFN-γ stimulated ERK1/2 and p38 activation and IL-6 production when compared to the vector control. Moreover, Raw264.7 macrophages experienced increased apoptosis under continuous IFN-γ stimulation and mPTPB expression more than tripled the amount of viable cells (as evidenced by the increased annexin V-negative/PI-negative cells from 7.5 to 24.5%) by activating Akt and blocking caspase 3 activity (Figure 4). Consistent with compound **4g** being an

dx.doi.org/10.1021/jm301781p | J. Med. Chem. 2013, 56, 832−842

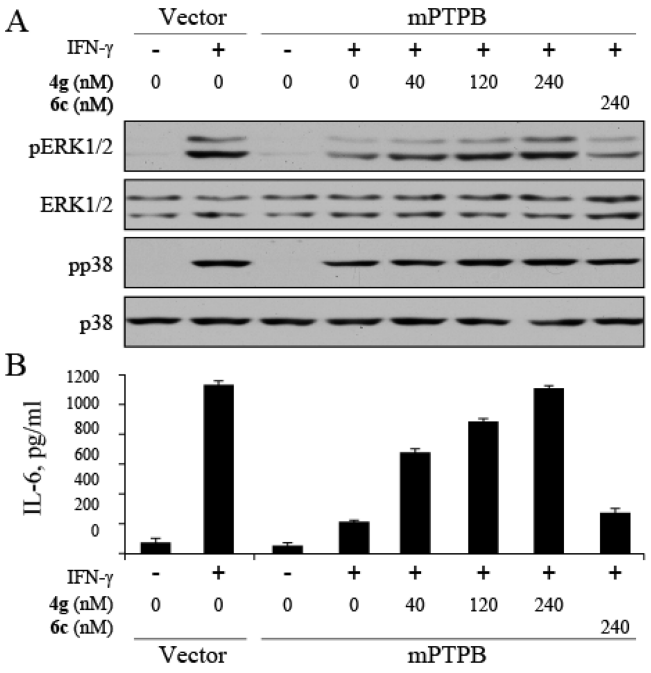

Figure 3. Compound **4g** restores ERK1/2 and p38 activity (A) and IL-6 production (B) in activated macrophages. Cells overexpressing mPTPB have decreased ERK1/2 and p38 activity and secrete lower levels of IL-6, and these can be reversed by treatment with the mPTPB inhibitor **4g** but not with a structurally related inactive compound **6c**. Data in panel B are expressed as means ± SD of three independent experiments.

mPTPB inhibitor, treatment of mPTPB expressing Raw264.7 macrophages with compound **4g** restored the IFN-γ induced activation of ERK1/2, p38, as well as IL6 production in a dose dependent manner (Figure 3). In addition, compound **4g** normalized Akt and caspase 3 activities and rescued the IFFN-γ induced apoptosis in mPTPB cells to the same extend as the vector control cells (Figure 4). To ensure that the cellular activity exerted by compound **4g** is not due to nonspecific effects, we also evaluated a structurally related but inactive compound **6c** (IC_{50} = 3.4 μM for mPTPB), which should not inhibit mPTPB and the mammalian PTPs at 240 nM concentration (Table 1). As expected, compound **6c** was unable to reverse the biochemical and functional perturbations introduced by mPTPB (Figures 3 and 4). Moreover, the observed cellular activity by compound **4g** also phenocopied those of several structurally unrelated small molecule mPTPB inhibitors.[12,13] Thus the ability of compound **4g** to block the mPTPB-mediated cellular signaling is unlikely due to off-target effects. Taken together, the results demonstrate that compound **4g** is highly efficacious in cell-based assays and capable of blocking mPTPB activity inside the cell.

CONCLUSION

Inhibitor specificity for the desired PTP is clearly an important goal in a PTP drug discovery program in order to avoid unintended off-target effect on other family members. Obtaining PTP inhibitors with optimal potency and selectivity has been difficult, due primarily to the high homology of the catalytic domains shared by all PTPs. In this study, we describe a medicinal chemistry optimization strategy that led to the discovery of a group of benzofuran salicylic acid-based mPTPB inhibitors that exhibit extremely high potency and selectivity.

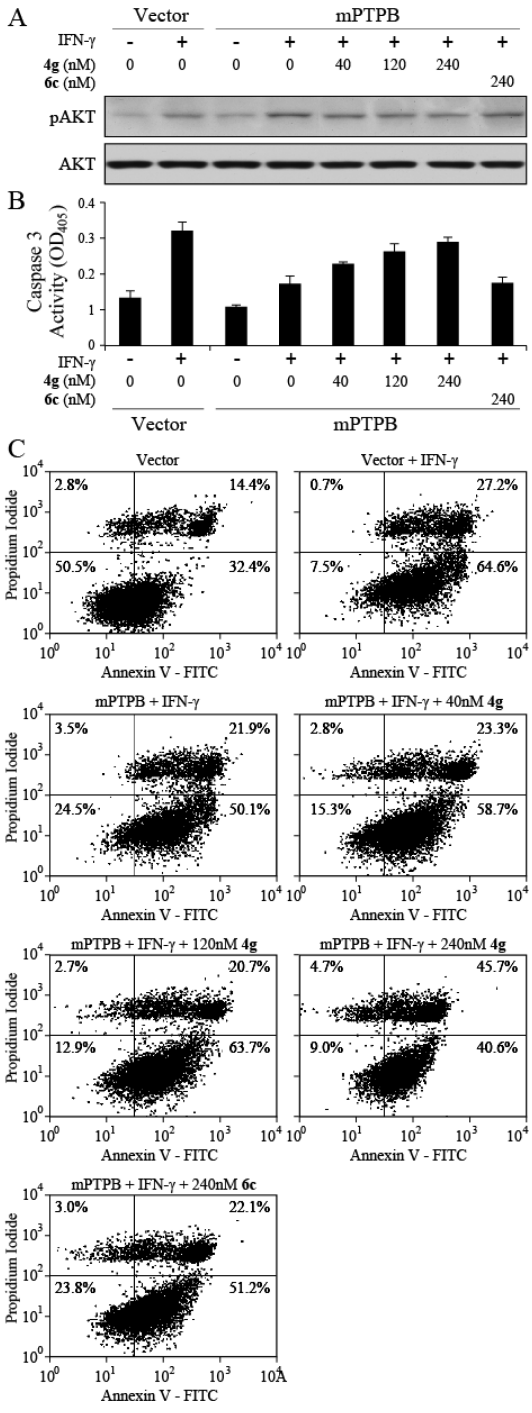

Figure 4. Inhibition of mPTPB with **4g** blocks Akt activation (A) and promotes caspase 3 activation (B) and macrophage apoptosis (C). Cells overexpressing mPTPB have increased Akt activity, lower caspase 3 activity, and higher propensity for cell survival, and these can be reversed by treatment with the mPTPB inhibitor **4g** but not with a structurally related inactive compound **6c**. Data in panel B are expressed as means ± SD of three independent experiments.

This is significant as it demonstrates the feasibility of acquiring specific PTP inhibitors by targeting unique areas within the active site pocket. Besides selectivity, bioavailability is another challenge in the development of PTP-based small-molecule therapeutics, because active site-directed inhibitors tend to mimic the pTyr substrate with substantial negative charges. Such molecules are generally not drug-like, with limited cell

dx.doi.org/10.1021/jm301781p | J. Med. Chem. 2013, 56, 832−842

membrane permeability. Our current and previous work[12,33,34] demonstrate that bicyclic salicylic acid pharmacophores are sufficiently polar to bind the PTP active site, yet remain capable of efficiently crossing cell membranes, offering PTP inhibitors with both high affinity and selectivity and excellent cellular efficacy. To this end, compound **4g** possesses highly efficacious cellular activity and is capable of reversing the altered host cell immune responses induced by the bacterial phosphatase. Overall, this class of compounds offers further opportunities to evaluate mPTPB inhibition as an anti-TB strategy.

EXPERIMENTAL SECTION

Materials. Recombinant mouse IFN-γ was purchased from PeproTech Inc. Anti-ERK1/2, antiphospho-ERK1/2, anti-p38, antiphospho-p38, and antiphospho-Akt473 antibodies were purchased from Cell Signaling. *p*-Nitrophenyl phosphate (*p*NPP) was purchased from Fluke Co. Dithiothreitol (DTT) was provided by Fisher (Fair Lawn, NJ). All reagents and solvents for organic synthesis were purchased from commercially available sources (FisherSci, Aldrich, Acros, Alfa Aesar, TCI).

General Procedures for Chemistry. ^{1}H NMR spectra were obtained on a Bruker 500 MHz NMR instrument. The chemical shifts were reported as δ ppm relative to TMS, using residual solvent peak as the reference unless otherwise noted. The following abbreviations were used to express the multiplicities: s = singlet; d = doublet; t = triplet; q = quartet; m = multiplet; br = broad. High-performance liquid chromatography (HPLC) purification was carried out on a Waters Delta 600 equipped with a Sunfire Prep C_{18} OBD column (30 × 150 mm, 5 μM) with methanol−water (both containing 0.1% TFA) as mobile phase (gradient: 50−100% methanol, flow 10 mL/min). All final compounds were obtained in highly purified form (>95%). Low-resolution mass spectra were obtained on an Agilent Technologies 6130 Quadrupole LC/MS. HRMS data were obtained at the Mass Spectrometry Facility at Indiana University Chemistry Department (http://msf.chem.indiana.edu) on a Waters/Macromass LCT (electrospray ionization ESI). All reactions were monitored by thin layer chromatography (TLC) carried out on Dynamic Adsorbents silica gel plates (0.25 mm thick, 60F254), visualized by using UV (254 nm). All compounds used for biological assays were purified by HPLC and are at least of 95% purity based on HPLC analytical results monitored with 254 nm wavelengths.

2,4-Dihydroxy-5-iodobenzoic Acid (7).[27] To a solution of 2,4-dihydroxybenzoic acid (20 g, 130 mmol) in acetic acid (150 mL) was added a solution of iodine monochloride (8.0 mL, 160 mmol) in acetic acid (100 mL) dropwise for 1 h at room temperature. The reaction mixture was stirred for another 4 h at room temperature. Acetic acid was removed in vacuum and water was added. The resulting precipitate was collected by filtration, washed with water and dried in vacuo to give compound **7** (33.1 g, 91%). ^{1}H NMR (500 MHz, $CDCl_3$) δ 12.45 (br, 1H), 11.31 (s, 1H), 8.10 (s, 1 H), 6.43 (s, 1H). Mass spectra (ESI): *m*/*e* 281 $(M + H)^+$.

7-Hydroxy-6-iodo-2,2-dimethyl-4*H*-benzo[*d*][1,3]dioxin-4-one (8).[28] To a suspension of 2,4-dihydroxy-5-iodobenzoic acid **7** (16.71 g, 59.7 mmol) in TFA (300 mL) were added TFAA (41.5 mL, 298 mmol) and dry acetone (35 mL, 478 mmol) dropwise at room temperature, and the mixture was stirred overnight. Then the homogeneous solution was concentrated to dry, and 500 mL of ethyl acetate was subsequently added. The organic layers were washed with water, the aqueous saturated $NaHCO_3$, water, and brine in stated order and dried over anhydrous Na_2SO_4, filtered, and concentrated. This crude material **8** (10.0 g, 52%) was then used directly in the next step.

6-Iodo-7-methoxy-2,2-dimethyl-4*H*-benzo[*d*][1,3]dioxin-4-one (9). To a solution of 7-hydroxy-6-iodo-2,2-dimethyl-4*H*-benzo-[*d*][1,3]dioxin-4-one **8** (34.66 g, 108 mmol) in DMSO (300 mL) were added K_2CO_3 (29.8 g, 216 mmol) and MeI (6.7 mL, 15.3 g, 108 mmol) at 0 °C. The reaction mixture was allowed to stir for 4 h at 25 °C and then diluted in a large amount of ether and washed with water and brine. The ether layer was then dried over $NaSO_4$, filtered,and concentrated. The crude material was then purified by column chromatography on silica gel to give the compound **9** (34.2 g, 95%). ^{1}H NMR (500 MHz, $CDCl_3$) δ 8.32 (s, 1H), 6.40 (s, 1H), 3.93 (s, 3H), 1.73 (s, 6H). Mass spectra (ESI): *m*/*e* 335 $(M + H)^+$.

7-Methoxy-2,2-dimethyl-6-(phenylethynyl)-4*H*-benzo[*d*]-[1,3]dioxin-4-one (10). A Schlenk flask was charged with 6-iodo-7-methoxy-2,2-dimethyl-4*H*-benzo[*d*][1,3]dioxin-4-one **9** (10.00 g, 29.9 mmol), phenylacetylene (1.2 equiv, 35.9 mmol), $Pd(PPh_3)_2Cl_2$ (3.0 mol %, 0.90 mmol), and CuI (6.0 mol %, 1.79 mmol). DMF (100 mL) was added and the flask was evacuated and backfilled with N_2 three times, and then Et_3N (4.0 equiv, 120 mmol) was added. The resulting reaction was stirred overnight at ambient temperature under N_2 overnight. The mixture was then diluted with 100 mL of water and 300 mL of ethyl acetate. After the phase cut, the organic layer was washed with water and brine. The organic layer was dried over Na_2SO_4 and filtered. Evaporation and chromatography on silica gel with the hexanes/ethyl acetate afforded the product **10** (7.46 g, 81%). ^{1}H NMR (500 MHz, $CDCl_3$) δ 8.08 (s, 1 H), 7.52 (m, 2H), 7.32−7.34 (m, 3H), 6.44 (s, 1H), 3.93 (s, 3H), 1.73 (s, 6H). ^{13}C NMR (125 M, $CDCl_3$) δ 165.91, 159.95, 157.72, 134.57, 131.50, 128.20, 123.07, 108.39, 106.58, 105.87, 98.95, 93.22, 83.67, 56.33, 25.72. Mass spectra (ESI): *m*/*e* 309 $(M + H)^+$.

6-Iodo-2,2-dimethyl-7-phenyl-4*H*-[1,3]dioxino[5,4-*f*]-benzofuran-4-one (11). The following procedure is a modification of our earlier procedure.[12] To a solution of 7-methoxy-2,2-dimethyl-6-(phenylethynyl)-4*H*-benzo[*d*][1,3]dioxin-4-one **10** (5 g, 16.22 mmol) in acetonitrile (100 mL) were added iodine (8.24 g, 32.44 mmol) and $NaHCO_3$ (2.7 g, 32.4 mmol). After the resulting mixture was stirred at 70 °C for 12 h, additional iodine (4.12 g, 16.22 mmol) and $NaHCO_3$ (1.36 g, 16.22 mmol) were added and the resulting reaction was allowed to stir for additional 12 h at 70 °C. Then the solvent was removed under reduced pressure and the residue was purified by column chromatography on silica gel using 6:1 hexanes/ethyl acetate to afford compound **11** (5.59 g, 82%). ^{1}H NMR (500 MHz, $CDCl_3$) δ 8.13 (m, 2H), 8.10 (s, 1H), 7.40−7.52 (m, 3H), 7.06 (s, 1H), 1.76 (s, 1H); ^{13}C NMR (125 M, $CDCl_3$) δ 161.11, 158.04, 154.74, 129.69, 129.13, 128.84, 128.61, 127.31, 123.93, 110.69, 106.52, 99.75, 60.50, 30.87, 25.86. Mass spectra (ESI): *m*/*e* 421 $(M + H)^+$.

General Procedure for Preparation of Compounds 14a−i via Sonogashira Coupling. A Schlenk flask was charged with 6-iodo-2,2-dimethyl-7-phenyl-4*H*-[1,3]dioxino[5,4-*f*]benzofuran-4-one (**11**) (1.0 mmol), $Pd(PPh_3)_2Cl_2$ (3.0 mol %, 0.03 mmol), and CuI (6.0 mol %, 0.06 mmol). DMF (5 mL) was added and the flask was evacuated and backfilled with N_2 three times. The alkyne (1.2 mmol) and Et_3N (4.0 equiv, 4.0 mmol) were then successively added. The resulting reaction was stirred at 40 °C under N_2 for the corresponding reaction times by TLC, after which time the reaction mixture was diluted with water (10 mL) and extracted with ethyl acetate (3 × 20 mL). The combined ethyl acetate layers were dried over Na_2SO_4, filtered, concentrated, and purified by silica gel flash chromatography using hexanes/ethyl acetate to elute the corresponding desired coupling product **14a−i**.

2,2-Dimethyl-7-phenyl-6-(phenylethynyl)-4*H*-[1,3]dioxino-[5,4-*f*]benzofuran-4-one (14a). 351 mg, yield 89%. ^{1}H NMR (500 MHz, $CDCl_3$) δ 8.37 (s, 1H), 8.28 (m, 2H), 7.62 (m, 2H), 7.50 (t, *J* = 7.8 Hz, 2H), 7.40 (m, 4H), 7.08 (s, 1H), 1.77 (s, 6H). ^{13}C NMR (125 M, $CDCl_3$) δ 161.38, 157.70, 157.43, 154.47, 131.61, 129.64, 129.34, 128.80, 128.78, 128.54, 125.90, 122.80, 122.38, 110.53, 106.51, 99.90, 99.33, 97.87, 79.79, 30.92, 25.86. Mass spectra (ESI): *m*/*e* 395 $(M + H)^+$.

6-((3-Fluorophenyl)ethynyl)-2,2-dimethyl-7-phenyl-4*H*-[1,3]dioxino[5,4-*f*]benzofuran-4-one (14b). 296 mg, yield 72%. ^{1}H NMR (500 MHz, $CDCl_3$) δ 8.36 (s, 1H), 8.25 (d, *J* = 7.6 Hz, 2H), 7.51 (t, *J* = 7.65 Hz, 2H), 7.44 (m, 1H), 7.40 (m, 2H), 7.31 (m, 1H), 7.12 (m, 1H), 7.09 (s, 1H), 1.78 (s, 6H). ^{13}C NMR (125 M, $CDCl_3$) δ 162.58 (d, *J* = 245.6 Hz), 161.47, 157.99, 157.80, 154.64, 130.30 (d, *J* = 8.4 Hz), 129.96, 129.32, 128.97, 127.65, 127.64, 126.07, 125.84, 124.70 (d, *J* = 9.2 Hz), 122.44, 118.43 (d, *J* = 22.9 Hz), 116.29 (d, *J* = 21.0 Hz), 110.73, 106.68, 100.09, 99.00, 96.54 (d, *J* = 3.5 Hz), 80.90, 25.99. Mass spectra (ESI): *m*/*e* 413 $(M + H)^+$.

dx.doi.org/10.1021/jm301781p | J. Med. Chem. 2013, 56, 832−842

6-((3-Chlorophenyl)ethynyl)-2,2-dimethyl-7-phenyl-4*H*-[1,3]dioxino[5,4-*f*]benzofuran-4-one (14c). 342 mg, yield 80%. ^{1}H NMR (500 MHz, $CDCl_3$) δ 8.35 (s, 1H), 8.23 (m, 2H), 7.59 (t, J = 1.8 Hz, 1H), 7.50 (m, 3H), 7.45 (m, 1H), 7.36 (m, 2H), 7.09 (s, 1H), 1.85 (s, 6H). ^{13}C NMR (125 M, $CDCl_3$) δ 161.31, 157.86, 157.66, 154.52, 134.40, 131.32, 129.83, 129.78, 129.74, 129.17, 129.03, 128.84, 125.94, 125.70, 124.47, 122.29, 110.61, 106.55, 99.96, 98.84, 96.26, 81.04, 25.86. Mass spectra (ESI): m/e 429 (M + H)$^+$.

6-((3-Methoxyphenyl)ethynyl)-2,2-dimethyl-7-phenyl-4*H*-[1,3]dioxino[5,4-*f*] benzofuran-4-one (14d). 301 mg, yield 71%. ^{1}H NMR (500 MHz, $CDCl_3$) δ 8.39 (s, 1H), 8.28 (m, 2H), 7.53 (t, J = 7.4 Hz, 2H), 7.45 (tt, J = 7.4 and 1.2 Hz, 1H), 7.33 (t, J = 8 Hz, 1H), 7.22 (dt, J = 7.5 and 1.2 Hz, 1H), 7.14 (m, 1H), 7.10 (s, 1H), 6.96 (ddd, J = 8.3, 2.55, and 0.85 Hz, 1H), 3.88 (s, 3H), 1.78 (s, 6H). ^{13}C NMR (125 M, $CDCl_3$) δ 161.55, 159.62, 157.85, 157.72, 154.62, 129.81, 129.75, 129.47, 128.93, 126.06, 126.01, 124.34, 123.92, 122.55, 116.42, 115.62, 110.68, 106.66, 100.05, 99.42, 97.88, 79.75, 55.56, 26.00. Mass spectra (ESI): m/e 425 (M + H)$^+$.

6-((2,4-Difluorophenyl)ethynyl)-2,2-dimethyl-7-phenyl-4*H*-[1,3]dioxino[5,4-*f*]benzofuran-4-one (14e). 297 mg, yield 69%. ^{1}H NMR (500 MHz, $CDCl_3$) δ 8.35 (s, 1H), 8.30 (m, 2H), 7.58 (m, 1H), 7.50 (m, 2H), 7.43 (m, 1H), 7.08 (s, 1H), 6.93 (m, 2H), 1.76 (s, 6H). ^{13}C NMR (125 M, $CDCl_3$) δ 163.19 (dd, J = 253.4 and 12.3 Hz), 163.07 (dd, J = 251.6 and 11.5 Hz), 161.33, 157.91, 157.67, 154.52, 134.08 (dd, J = 9.7 and 2.3 Hz), 129.83, 129.10, 128.80, 125.94, 125.63, 122.29, 111.87 (dd, J = 21.8 and 3.6 Hz), 110.63, 107.92 (dd, J = 16.0 and 3.8 Hz), 106.55, 104.49 (t, J = 25.5 Hz), 99.96, 98.80, 90.30, 84.82, 25.87. Mass spectra (ESI): m/e 431 (M + H)$^+$.

6-((3,5-Difluorophenyl)ethynyl)-2,2-dimethyl-7-phenyl-4*H*-[1,3]dioxino[5,4-*f*]benzofuran-4-one (14f). 314.2 mg, yield 73%. ^{1}H NMR (500 MHz, $CDCl_3$) δ 8.34 (s, 1H), 8.24 (m, 2H), 7.53 (t, J = 7.85 Hz, 2H), 7.47 (m, 1H), 7.12 (m, 2H), 7.10 (s, 1H), 6.87 (m, 1H), 1.78 (s, 6H). ^{13}C NMR (125 M, $CDCl_3$) δ 163.01 (dd, J = 248.1 and 13.3 Hz), 161.42, 158.46, 157.82, 154.73, 130.17, 129.21, 129.04, 126.15, 125.66, 125.51 (t, J = 11.7 Hz), 122.40, 114.67 (dd, J = 20.3 and 6.8 Hz), 110.86, 106.74, 105.11 (t, J = 25.2 Hz), 98.60, 95.40 (t, J = 3.7 Hz), 82.06, 26.01. Mass spectra (ESI): m/e 431 (M + H)$^+$.

2,2-Dimethyl-7-phenyl-6-((3-(trifluoromethyl)phenyl)-ethynyl)-4*H*-[1,3]dioxino[5,4-*f*]benzofuran-4-one (14g). 300 mg, yield 65%. ^{1}H NMR (500 MHz, $CDCl_3$) δ 8.36 (s, 1H), 8.26 (m, 2H), 7.85 (s, 1H), 7.78 (d, J = 7.7 Hz, 1H), 7.64 (d, J = 7.7 Hz, 1H), 7.52 (m, 3H), 7.46 (m, 1H), 7.09 (s, 1H), 1.77 (s, 6H). ^{13}C NMR (125 M, $CDCl_3$) δ 161.32, 158.07, 157.69, 154.57, 134.70, 131.23 (q, J = 32.5 Hz), 129.93, 129.15, 129.13, 128.88, 128.26 (q, J = 4.0 Hz), 126.00, 125.65, 125.31 (q, J = 3.7 Hz), 124.76, 123.74, 122.59, 110.67, 106.59, 100.01, 98.71, 96.03, 81.45, 25.87. Mass spectra (ESI): m/e 463 (M + H)$^+$.

2,2-Dimethyl-7-phenyl-6-((4-(trifluoromethoxy)phenyl)-ethynyl)-4*H*-[1,3]dioxino[5,4-*f*]benzofuran-4-one (14h). 426 mg, yield 89%. ^{1}H NMR (500 MHz, $CDCl_3$) δ 8.35 (s, 1H), 8.25 (m, 2H), 7.64 (dt, J = 8.8 and 2.0 Hz, 2H), 7.50 (t, J = 7.9 Hz, 2H), 7.44 (m, 1H), 7.27 (d, J = 6.8 Hz, 2H), 7.09 (s, 1H), 1.78 (s, 6H). ^{13}C NMR (125 M, $CDCl_3$) δ 161.37, 157.78, 157.69, 154.53, 149.28, 149.26, 133.14, 129.82, 129.23, 128.84, 125.94, 125.74, 122.30, 121.56, 121.07, 120.41 (q, J = 256.3 Hz), 110.61, 106.58, 99.98, 98.94, 96.26, 80.73, 25.87. Mass spectra (ESI): m/e 478 (M + H)$^+$.

2,2-Dimethyl-6-((4-phenoxyphenyl)ethynyl)-7-phenyl-4*H*-[1,3]dioxino[5,4-*f*]benzofuran-4-one (14i). 462 mg, yield 95%. ^{1}H NMR (500 MHz, $CDCl_3$) δ 8.38 (s, 1H), 8.28 (d, J = 7.3 Hz, 2H), 7.57 (dt, J = 8.7 and 2.0 Hz, 2H), 7.39 (m, 3H), 7.17 (t, J = 8.7 Hz, 1H), 7.08 (m, 3H), 7.03 (tt, J = 8.7 and 2.0 Hz, 2H), 1.77 (s, 6H). ^{13}C NMR (125 M, $CDCl_3$) δ 161.40, 158.15, 157.71, 157.26, 156.27, 154.46, 133.27, 129.95, 129.59, 129.39, 128.78, 125.95, 125.86, 124.03, 122.39, 119.58, 118.44, 117.24, 110.51, 106.51, 99.89, 99.44, 97.50, 79.15, 25.87. Mass spectra (ESI): m/e 487 (M + H)$^+$.

General Procedure for Preparation of Compounds 2, 3, and 4a−i. To a solution of **14a−i** (0.5 mmol) in THF (3 mL), KOH (400 mg, 7.14 mmol) in water (1 mL) was added. The obtained mixture was refluxed for 2 h, then acidified with 3 M HCl and extracted with ethyl acetate. The organic layers were dried over anhydrous Na_2SO_4, filtered, and concentrated under reduced pressure. The residue was purified by HPLC to furnish the corresponding products **4a−i**. Yield 70−90%. Compounds **2** and **3** were prepared from compound **11** directly via two steps.

6-Hydroxy-2-phenyl-3-(phenylethynyl)benzofuran-5-carboxylic Acid (4a). ^{1}H NMR (500 MHz, DMSO-d_6) δ 8.17 (d, J = 7.6 Hz, 2H), 8.08 (s, 1H), 7.68 (m, 2H), 7.58 (t, J = 7.6 Hz, 2H), 7.50 (m, 4H), 7.20 (s, 1H). ^{13}C NMR (125 M, DMSO-d_6) δ 171.99, 160.58, 156.94, 155.98, 131.41, 129.69, 129.18, 129.08, 128.88, 128.75, 125.23, 121.95, 121.80, 121.37, 110.50, 99.08, 98.30, 97.31, 79.88. Mass spectra (ESI): m/e 355 (M + H)$^+$.

3-((3-Fluorophenyl)ethynyl)-6-hydroxy-2-phenylbenzofuran-5-carboxylic Acid (4b). ^{1}H NMR (500 MHz, DMSO-d_6) δ 8.15 (d, J = 7.7 Hz, 2H), 8.09 (s, 1H), 7.58 (t, J = 7.7 Hz, 2H), 7.50 (m, 4H), 7.33 (m, 1H), 7.21 (s, 1H). Mass spectra (ESI): m/e 373 (M + H)$^+$.

3-((3-Chlorophenyl)ethynyl)-6-hydroxy-2-phenylbenzofuran-5-carboxylic Acid (4c). ^{1}H NMR (500 MHz, DMSO-d_6) δ 8.11 (d, J = 7.6 Hz, 2H), 8.05 (s, 1H), 7.70 (s, 1H), 7.55 (m, 4H), 7.46 (m, 2H), 7.15 (s, 1H). ^{13}C NMR (125 M, DMSO-d_6) δ 171.99, 160.60, 156.89, 156.41, 133.46, 130.69, 130.66, 130.14, 129.82, 129.21, 129.11, 128.60, 125.33, 123.89, 121.90, 121.18, 110.61, 99.06, 97.91, 95.66, 81.22. Mass spectra (ESI): m/e 389 (M + H)$^+$.

6-Hydroxy-3-((3-methoxyphenyl)ethynyl)-2-phenylbenzofuran-5-carboxylic Acid (4d). ^{1}H NMR (500 MHz, DMSO-d_6) δ 8.17(d, J = 7.5 Hz, 2H), 8.09 (s, 1H), 7.58 (t, J = 7.5 Hz, 2H), 7.48 (t, J = 7.4 Hz, 1H), 7.39 (t, J = 7.8 Hz, 1H), 7.22 (m, 3H), 7.05 (dd, J = 8.2 and 2.0 Hz, 1H), 3.82 (s, 3H). ^{13}C NMR (125 M, DMSO-d_6) δ 171.99, 160.58, 159.30, 156.98, 156.17, 130.08, 129.80, 129.15, 128.74, 125.29, 123.88, 122.96, 121.89, 121.34, 116.15, 115.67, 110.58, 99.17, 98.27, 97.25, 79.70, 55.31. Mass spectra (ESI): m/e 385 (M + H)$^+$.

3-((2,4-Difluorophenyl)ethynyl)-6-hydroxy-2-phenylbenzofuran-5-carboxylic Acid (4e). ^{1}H NMR (500 MHz, DMSO-d_6) δ 8.17 (d, J = 7.4 Hz, 2H), 8.06 (s, 1H), 7.82 (m, 1H), 7.54 (t, J = 7.4 Hz, 2H), 7.46 (m, 2H), 7.20 (m, 2H). ^{13}C NMR (125 M, DMSO-d_6) δ 171.92, 162.58 (dd, J = 248.8 and 23.0 Hz), 162.49 (dd, J = 248.4 and 24.1 Hz), 160.63, 156.90, 156.26, 134.55 (d, J = 10.1 Hz), 129.88, 129.10, 128.54, 125.21, 121.76, 121.12, 112.49 (d, J = 21.9 Hz), 110.66, 107.12 (d, J = 15.5 Hz), 104.80 (t, J = 25.6 Hz), 99.52, 99.15, 97.84, 89.83, 84.87. Mass spectra (ESI): m/e 391 (M + H)$^+$.

3-((3,5-Difluorophenyl)ethynyl)-6-hydroxy-2-phenylbenzofuran-5-carboxylic Acid (4f). ^{1}H NMR (500 MHz, DMSO-d_6) δ 8.11(d, J = 7.5 Hz, 2H), 8.06 (s, 1H), 7.56 (t, J = 7.5 Hz, 2H), 7.47 (m, 1H), 7.38 (m, 3H), 7.15 (s, 1H). ^{13}C NMR (125 M, DMSO-d_6) δ 171.99, 162.38 (d, J = 245.7 Hz), 162.27 (d, J = 245.7 Hz), 160.61, 156.84 (d, J = 9.8 Hz), 129.93, 129.17, 128.47, 125.40, 124.74 (t, J = 12.0 Hz), 121.98, 121.05, 114.68 (dd, J = 20.3 and 7.0 Hz), 110.64, 105.36 (t, J = 25.7 Hz), 99.09, 97.55, 94.80, 82.00. Mass spectra (ESI): m/e 391 (M + H)$^+$.

6-Hydroxy-2-Phenyl-3-((3-(trifluoromethyl)phenyl)ethynyl)-benzofuran-5-carboxylic Acid (4g). ^{1}H NMR (500 MHz, DMSO-d_6) δ 8.11 (d, J = 7.5 Hz, 2H), 8.06 (s, 1H), 7.95 (s, 1H), 7.90 (d, J = 7.7 Hz, 1H), 7.79 (d, J = 7.7 Hz, 1H), 7.78 (t, J = 7.7 Hz, 1H), 7.54 (t, J = 7.4 Hz, 2H), 7.46 (t, J = 7.4 Hz, 1H), 7.14 (s, 1H). ^{13}C NMR (125 M, DMSO-d_6) δ 171.99, 160.60, 156.89, 156.55, 135.30, 130.01, 129.84, 129.74 (q, J = 32.0 Hz), 129.08, 128.58, 127.68 (q, J = 3.7 Hz), 125.54 (q, J = 3.7 Hz), 125.37, 123.70 (q, J = 271 Hz), 123.09, 121.95, 121.14, 110.59, 99.05, 97.83, 95.49, 81.56. Mass spectra (ESI): m/e 423 (M + H)$^+$.

6-Hydroxy-2-phenyl-3-((4-(trifluoromethoxy)phenyl)-ethynyl)benzofuran-5-carboxylic Acid (4h). ^{1}H NMR (500 MHz, DMSO-d_6) δ 8.15 (d, J = 7.5 Hz, 2H), 8.07 (s, 1H), 7.79 (d, J = 8.8 Hz, 2H), 7.56 (t, J = 7.5 Hz, 2H), 7.46 (m, 3H), 7.19 (s, 1H). Mass spectra (ESI): m/e 439 (M + H)$^+$.

6-Hydroxy-3-((4-phenoxyphenyl)ethynyl)-2-phenylbenzofuran-5-carboxylic Acid (4i). ^{1}H NMR (500 MHz, DMSO-d_6) δ 11.70 (br, 1H), 8.16 (d, J = 7.5 Hz, 2H), 8.06 (s, 1H), 7.67 (d, J = 8.7 Hz, 2H), 7.56 (t, J = 7.5 Hz, 2H), 7.45 (m, 3H), 7.22 (m, 2H), 7.10 (d, J = 7.8 Hz, 2H), 7.04 (d, J = 8.7 Hz, 2H). ^{13}C NMR (125 M, DMSO-d_6) δ 171.99, 160.56, 157.75, 156.97, 155.80, 155.61, 133.45, 130.26, 129.68, 129.12, 128.79, 125.19, 124.31, 121.83, 121.43, 119.48, 118.37,

dx.doi.org/10.1021/jm301781p | J. Med. Chem. 2013, 56, 832−842

116.48, 110.49, 99.13, 98.44, 97.01, 79.23. Mass spectra (ESI): *m/e* 447 $(M + H)^+$.

3-Ethisterone-6-hydroxy-2-phenylbenzofuran-5-carboxylic Acid (2). ^{1}H NMR (500 MHz, DMSO-d_6) δ 11.7 (br, 1H), 8.16 (m, 2H), 8.09 (s, 1H), 7.51 (t, J = 7.8 Hz, 2H), 7.46 (t, J = 7.8 Hz, 1H), 7.22 (s, 1H), 5.62 (s, 1H), 2.56 (s, 2H), 2.39−2.2 (m, 4H), 2.14−2.02 (m, 2H), 1.92 (m, 1H), 1.83 (m, 1H), 1.76 (m, 3H), 1.57 (m, 4H), 1.38 (m, 2H), 1.14 (s, 3H), 0.90 (m, 2H), 0.87 (s, 3H). ^{13}C NMR (125 M, DMSO-d_6) δ 197.93, 172.08, 170.60, 160.51, 156.92, 155.05, 129.52, 128.87, 128.80, 125.00, 123.21, 121.93, 121.86, 110.34, 103.48, 99.06, 98.69, 78.96, 74.77, 53.43, 50.21, 46.74, 40.36, 38.11, 35.56, 35.03, 33.53, 32.74, 31.84, 31.41, 22.78, 20.34, 16.88, 12.75.

6-Hydroxy-3-(3-hydroxyprop-1-yn-1-yl)-2-phenylbenzofuran-5-carboxylic Acid (3). ^{1}H NMR (500 MHz, DMSO-d_6) δ 8.18 (d, J = 7.4 Hz, 2H), 8.07 (s, 1H), 7.57 (t, J = 7.4 Hz, 2H), 7.49 (t, J = 7.4 Hz, 1H), 7.24 (s, 1H), 4.50 (s, 2H). ^{13}C NMR (125 M, DMSO-d_6) δ 161.0, 157.37, 156.15, 130.18, 129.58, 129.21, 125.60, 122.27, 100.00, 99.62, 99.22, 98.77, 74.50, 50.26.

(*Z*)-3-(3,5-Difluorostyryl)-6-hydroxy-2-phenylbenzofuran-5-carboxylic Acid (5a). To a stirred solution of 3-((3,5-difluorophenyl)ethynyl)-6-hydroxy-2-phenylbenzofuran-5-carboxylic acid **4f** (126 mg, 0.32 mmol) in MeOH/THF (1/1, 2 mL) was added 5% Pd/$BaSO_4$ (15 mg), and the mixture was allowed to stir for 12 h at room temperature under H_2 atmosphere. The mixture was filtered through Celite pad, and the filtrate was concentrated under reduced pressure. The residue was purified by HPLC to furnish compound **5a** (110 mg, 88%). ^{1}H NMR (500 MHz, DMSO-d_6) δ 7.82 (d, J = 7.35 Hz, 2H), 7.52 (t, J = 7.45 Hz, 2H), 7.44 (m, 1H), 7.30 (s, 1H), 7.16 (s, 1H), 7.03 (m, 1H), 6.98 (d, J = 12 Hz, 1H), 6.92 (m, 2H), 6.86 (d, J = 12 Hz, 1H). ^{13}C NMR (125 M, DMSO-d_6) δ 171.99, 162.25 (d, J = 244.3 Hz), 161.14 (d, J = 244.4 Hz), 159.80, 157.84, 152.03, 140.26 (t, J = 9.9 Hz), 131.23, 129.48, 129.15, 129.04, 126.37, 123.21, 121.81, 119.46, 112.43, 111.38 (dd, J = 20.4 and 7.0 Hz), 109.54, 102.99 (t, J = 26.0 Hz), 98.79. Mass spectra (ESI): *m/e* 393 $(M + H)^+$.

(*Z*)-6-Hydroxy-2-phenyl-3-(4-(trifluoromethoxy)styryl)-benzofuran-5-carboxylic Acid (5b). To a stirred solution of 6-hydroxy-2-phenyl-3-((4-(trifluoromethoxy)phenyl)ethynyl)-benzofuran-5-carboxylic acid **4h** (98 mg, 0.22 mmol) in MeOH/THF (1/1, 2 mL) was added 5% Pd/$BaSO_4$ (15 mg), and the mixture was allowed to stir for 12 h at room temperature under H_2 atmosphere. The mixture was filtered through Celite pad, and the filtrate was concentrated under reduced pressure. The residue was purified by HPLC to furnish compound **5b** (90 mg, 92%). ^{1}H NMR (500 MHz, DMSO-d_6) δ 11.6 (br, 1H), 7.85 (d, J = 7.4 Hz, 1H), 7.53 (t, J = 8.0 Hz, 2H), 7.45 (t, J = 7.4 Hz, 1H), 7.37 (t, J = 8.7 Hz, 2H), 7.25 (s,k 1H), 7.16 (m, 3H), 7.05 (d, J = 12 Hz, 1H), 6.80 (d, J = 12 Hz, 1H). ^{13}C NMR (125 M, DMSO-d_6) δ 172.03, 159.76, 157.88, 151.67, 147.48, 135.95, 132.08, 130.25, 129.63, 129.02, 128.99, 126.22, 123.41, 120.83, 120.17, 119.96 (q, J = 255.1 Hz), 119.54, 112.91, 109.37, 98.71. Mass spectra (ESI): *m/e* 441 $(M + H)^+$.

General Procedure for Preparation of Compounds 6a−d. To a stirred solution of appropriate carboxylic acid (0.30 mmol) in MeOH/THF (1/1, 2 mL) was added 10% Pd/C (15 mg), and the mixture was allowed to stir for 12 h at room temperature under H_2 atmosphere. The mixture was filtered through Celite pad, and the filtrate was concentrated under reduced pressure. The residue was purified by HPLC to furnish desired compounds **6a−d** in 90−95% yield.

3-(3-Fluorophenethyl)-6-hydroxy-2-phenylbenzofuran-5-carboxylic Acid (6a). ^{1}H NMR (500 MHz, DMSO-d_6) δ 11.70 (br, 1H), 8.03 (s, 1H), 7.64 (d, J = 7.35 Hz, 2H), 7.50 (t, J = 7.7 Hz, 2H), 7.40 (t, J = 7.4 Hz, 1H), 7.25 (m, 1H), 7.11 (s, 1H), 7.09 (m, 1H), 7.01 (d, J = 7.7 Hz, 1H), 6.97 (m, 1H), 3.17 (t, J = 7.4 Hz, 2H), 2.98 (t, J = 7.4 Hz, 2H). Mass spectra (ESI): *m/e* 377 $(M + H)^+$.

6-Hydroxy-2-phenyl-3-(3-(trifluoromethyl)phenethyl)-benzofuran-5-carboxylic Acid (6b). ^{1}H NMR (500 MHz, DMSO-d_6) δ 11.65 (br, 1H), 7.96 (s, 1H), 7.61 (d, J = 7.3 Hz, 2H), 7.54 (s, 1H), 7.51 (m, 1H), 7.47 (m, 4H), 7.40 (m, 3H), 7.10 (s, 1H), 3.20 (t, J = 7.4 Hz, 2H), 3.07 (t, J = 7.4 Hz, 2H). Mass spectra (ESI): *m/e* 427 $(M + H)^+$.

6-Hydroxy-2-phenyl-3-(4-(trifluoromethoxy)phenethyl)-benzofuran-5-carboxylic Acid (6c). ^{1}H NMR (500 MHz, DMSO-d_6) δ 11.65 (br, 1H), 7.97 (s, 1H), 7.61 (d, J = 7.3 Hz, 2H), 7.48 (t, J = 7.7 Hz, 2H), 7.40 (m, 1H), 7.29 (d, J = 8.6 Hz, 2H), 7.18 (d, J = 8.0 Hz, 2H), 7.11 (s, 1H), 3.17 (t, J = 7.5 Hz, 2H), 3.00 (t, J = 7.5 Hz, 2H). Mass spectra (ESI): *m/e* 443 $(M + H)^+$.

6-Hydroxy-3-(4-phenoxyphenethyl)-2-phenylbenzofuran-5-carboxylic Acid (6d). ^{1}H NMR (500 MHz, DMSO-d_6) δ 11.65 (br, 1H), 7.97 (s, 1H), 7.65 (d, J = 7.4 Hz, 2H), 7.50 (t, J = 7.7 Hz, 2H), 7.41 (t, J = 7.4 Hz, 1H), 7.32 (t, J = 8.0 Hz, 2H), 7.17 (d, J = 8.5 Hz, 2H), 7.11 (s, 1H), 7.08 (t, J = 7.4 Hz, 1H), 6.84 (m, 1H), 3.17 (t, J = 7.4 Hz, 2H), 2.97 (t, J = 7.4 Hz, 2H). ^{13}C NMR (125 M, DMSO-d_6) δ 172.39, 159.82, 157.49, 157.24, 154.56, 150.66, 136.20, 130.09, 129.95, 129.86, 128.94, 128.46, 126.11, 122.91, 122.80, 122.11, 119.00, 117.83, 115.26, 109.28, 98.44, 34.12, 25.54. Mass spectra (ESI): *m/e* 451 $(M + H)^+$.

Cell Culture and Transfection. Raw264.7 mouse macrophages were cultured in Dulbecco's modified Eagle's medium (DMEM) supplemented with 10% FBS (Invitrogen), penicillin (50 units/mL), and streptomycin (50 μg/mL) under a humidified atmosphere containing 5% CO_2 at 37 °C. Transfected Raw264.7 cells (Vector, WT-mPTPB) were seeded in a 12-well plate at a density of 4×10^4 cells/well. The following day cells were treated with mPTPB inhibitor **4g** for 1 h and stimulated with IFN-γ (200 U/ml) for 1 h. Cells were then washed with ice-cold phosphate buffered saline, and lysed with lysis buffer on ice for 30 min. Cell lysates were cleared by centrifugation at 13 000 rpm for 15 min. The phosphorylation of ERK1/2, p38, and Akt was detected by Western blotting.

IL-6 Enzyme-Linked Immunosorbent Assay (ELISA). Transfected Raw264.7 cells (Vector, WT-mPTPB) were seeded in a 12-well plate at a density of 4×10^4 cells/well. The following day cells were treated with mPTPB inhibitor **4g** for 1 h and then were left unstimulated or stimulated for 24 h with IFN-γ (200 U/ml). After 24 h incubation, supernatants were collected, cleared by centrifugation, and assayed for IL-6 release using mouse IL-6 ELISA kit (eBioscience) and a plate reader.

Caspase Activity Assay. mPTPB transfected Raw264.7 cells were treated with either compound **4g** or the negative control **6c** for 1 h, then stimulated with IFN-γ (200U/ml). After 24 h, about 4×10^5 cells were collected. The substrate Ac-DEVD-pNA (Sigma) was used to measure caspase-3 activity following the described procedures.[35] Briefly, the collected cells were washed in ice-cold PBS, and lysed in 50 μL of caspase lysis buffer (25 mM HEPES, pH 7.5, 5 mM EDTA, 5 mM $MgCl_2$, 10 mM DTT, 10 μg/mL each of pepstatine and leupeptin, 0.5% TX-100, and 2 mM PMSF). Cells were kept on ice for 20 min with occasional mixing. The lysates were then centrifuge at 13 000*g* for 15 min at 4 °C. Protein concentration of the supernatant was determined using the Bradford method (Bio-Rad). Subsequently, the supernatant containing 50 μg of protein was diluted into a final volume of 200 μL with the assay buffer (50 mM HEPES, 10% sucrose, 0.1% CHAPS, and 10 mM DTT) containing 100 μM of the substrate Ac-DEVD-pNA and incubated for 2hr in a 96-well plate at 37 °C. The cleavage of the substrate by caspase-3 in the lysate released pNA, which was determined by measuring the absorbance at 405 nm using a plate reader spectrophotometer.

Flow Cytometric Analysis. mPTPB transfected Raw264.7 cells were treated with **4g** or the negative control **6c** for 1 h, and then stimulated with IFN-γ (200U/ml). After 24 h, about 4×10^5 cells were harvested by resuspending in the Cell Dissociation Buffer (GIBCOTM, Invitrogen Corporation) and gently scraped into a 15 mL centrifuge tube. The collected cells were stained either with annexinV-APC and PI proceeding with the protocol of Annexin V-APC Apoptosis Detection Kit (BD PharmingenTM). Briefly, cells were washed twice with cold PBS and then were resuspended in 500 μL of 1x binding buffer. A totalof 100 μL of solution was transferred to a 5 mL culture tube. Five microliters of Annexin V-APC and 5 μL of PI were added into the solution. The solution was gently vortexed and incubated for 15 min at room temperature in the dark. Then 400 μL of 1x binding buffer was added into each tube. Each group of samples was

analyzed using a BD FACSArray Bioanalyzer. The data were analyzed using CellQuest software (BD Biosciences).

Kinetic Analysis of mPTPB Inhibition. The phosphatase activity of mPTPB was assayed using *p*-nitrophenyl phosphate (*p*NPP) as a substrate at 25 °C in 50 mM 3,3-dimethylglutarate buffer, pH 7.0, containing 1 mM EDTA with an ionic strength of 0.15 M adjusted by NaCl. Compounds exhibiting more than 50% of inhibitory activity against mPTPB were selected for IC_{50} measurement. The reaction was started by the addition of 5 μL of the enzyme to 195 μL of reaction mixture containing 2.5 mM (the K_m value) of *p*NPP and various concentrations of the inhibitor. The reaction was quenched after 5 min by the addition of 50 μL of 5N NaOH, and then 200 μL of reaction mixture was transferred to a 96-well plate. The nonenzymatic hydrolysis of *p*NPP was corrected by measuring the control without the addition of enzyme. The amount of product *p*-nitrophenol was determined from the absorbance at 405 nm detected by a Spectra MAX340 microplate spectrophotometer (Molecular Devices) using a molar extinction coefficient of 18 000 M^{-1} cm^{-1}. IC_{50} values were calculated by fitting the absorbance at 405 nm versus inhibitor concentration to the following equation:

$$A_I/A_0 = IC_{50}/(IC_{50} + [I])$$

where A_I is the absorbance at 405 nm of the sample in the presence of inhibitor; A_0 is the absorbance at 405 nm in the absence of inhibitor; and [I] is the concentration of the inhibitor.

For selectivity studies, the PTPs, including mPTPA, PTP1B, TC-PTP, SHP1, SHP2, FAP1, Lyp, PTP-MEG2, HePTP, PTPα, LAR, CD45, PTPγ, VHR, Laforin, VHX, Cdc14A, and LMWPTP PTP were expressed and purified from *E. coli*. The inhibition assay for these PTPs were performed under the same conditions as mPTPB except using a different *p*NPP concentration corresponding to the K_m of the PTP studied. Inhibitor concentrations used for IC_{50} measurements cover the range from 0.2 to 5× of the IC_{50} value.

AUTHOR INFORMATION

Corresponding Author

*Phone: (317) 274-8025. E-mail: zyzhang@iupui.edu.

Notes

The authors declare no competing financial interest.

ACKNOWLEDGMENTS

This work was supported by National Institutes of Health Grants R56 AI090829 and CA126937.

REFERENCES

(1) Hunter, T. The phosphorylation of proteins on tyrosine: its role in cell growth and disease. *Philos. Trans. R. Soc., B.* **1998**, *353*, 583–605.

(2) Zhang, Z.-Y. Protein tyrosine phosphatases: prospects for therapeutics. *Curr. Opin. Chem. Biol.* **2001**, *5*, 416–423.

(3) Ventura, J. J.; Nebreda, A. R. Protein kinases and phosphatases as therapeutic targets in cancer. *Clin. Transl. Oncol.* **2006**, *8*, 153–160.

(4) Jänne, P. A.; Gray, N.; Settleman, J. Factors underlying sensitivity of cancers to small-molecule kinase inhibitors. *Nat. Rev. Drug Discovery* **2009**, *8*, 709–723.

(5) Raviglione, M. C. XDR-TB: entering the post-antibiotic era? *Int. J. Tuberc. Lung Dis.* **2006**, *10*, 1185–1187.

(6) Gandhi, N. R.; Nunn, P.; Dheda, K.; Schaaf, H. S.; Zignol, M.; Soolingen, D. V.; Jensen, P.; Bayona, J. Multidrug-resistant and extensively drug-resistant tuberculosis: a threat to global control of tuberculosis. *Lancet* **2010**, *375*, 1830–1843.

(7) Zahrt, T. C. Molecular mechanisms regulating persistent *Mycobacterium tuberculosis* infection. *Microbes Infect.* **2003**, *5*, 159–167.

(8) Clatworthy, A. E.; Pierson, E.; Hung, D. T. Targeting virulence: a new paradigm for antimicrobial therapy. *Nat. Chem. Biol.* **2007**, *3*, 541–548.

(9) Singh, R.; Rao, V.; Shakila, H.; Gupta, R.; Khera, A.; Dhar, N.; Singh, A.; Koul, A.; Singh, Y.; Naseema, M.; Narayanan, P. R.; Paramasivan, C. N.; Ramanathan, V. D.; Tyagi, A. K. Disruption of mptpB impairs the ability of *Mycobacterium tuberculosis* to survive in guinea pigs. *Mol. Microbiol.* **2003**, *50*, 751–762.

(10) Singh, R.; Singh, A.; Tyagi, A. K. Deciphering the genes involved in pathogenesis of Mycobacterium tuberculosis. *Tuberculosis* **2005**, *85*, 325–335.

(11) Koul, A.; Herget, T.; Klebl, B.; Ullrich, A. Interplay between mycobacteria and host signalling pathways. *Nat. Rev. Microbiol.* **2004**, *2*, 189–202.

(12) Zhou, B.; He, Y.; Zhang, X.; Xu, J.; Luo, Y.; Wang, Y.; Franzblau, S. G.; Yang, Z.; Chan, R. J.; Liu, Y.; Zheng, J.; Zhang, Z.-Y. Targeting Mycobacterium Protein Tyrosine Phosphatase B for Anti-Tuberculosis Agents. *Proc. Natl. Acad. Sci. U.S.A.* **2010**, *107*, 4573–4578.

(13) Chen, L.; Zhou, B.; Zhang, S.; Wu, L.; Wang, Y.; Franzblau, S. G.; Zhang, Z.-Y. Identification and characterization of small molecule inhibitors of mPTPB, an essential virulent phosphatase from *Mycobacterium tuberculosis*. *ACS Med. Chem. Lett.* **2010**, *1*, 355–359.

(14) Leemans, J. C.; Juffermans, N. P.; Florquin, S.; van Rooijen, N.; Vervoordeldonk, M. J.; Verbon, A.; van Deventer, S. J.; van der Poll, T. Depletion of alveolar macrophages exerts protective effects in pulmonary tuberculosis in mice. *J. Immunol.* **2001**, *166*, 4604–4611.

(15) Schaible, U. E.; Winau, F.; Sieling, P. A.; Fischer, K.; Collins, H. L.; Hagens, K.; Modlin, R. L.; Brinkmann, V.; Kaufmann, S. H. Apoptosis facilitates antigen presentation to T lymphocytes through MHC-I and CD1 in tuberculosis. *Nat. Med.* **2003**, *9*, 1039–1046.

(16) Keane, J.; Balcewicz-Sablinska, M. K.; Remold, H. G.; Chupp, G. L.; Meek, B. B.; Fenton, M. J.; Kornfeld, H. Infection by Mycobacterium tuberculosis promotes human alveolar macrophage apoptosis. *Infect. Immun.* **1997**, *65*, 298–304.

(17) Lee, J.; Kornfeld, H. Interferon-γ Regulates the Death of M. tuberculosis-Infected Macrophages. *J. Cell Death* **2010**, *3*, 1–11.

(18) Behar, S. M.; Martin, C. J.; Booty, M. G.; Nishimura, T.; Zhao, X.; Gan, H.-X.; Divangahi, M.; Remold, H. G. Apoptosis is an innate defense function of macrophages against Mycobacterium tuberculosis. *Mucosal Immunol.* **2011**, *4*, 279–287.

(19) Beresford, N. J.; Mulhearn, D.; Szczepankiewicz, B.; Liu, G.; Johnson, M. E.; Fordham-Skelton, A.; Abad-Zapatero, C.; Cavet, J. S.; Tabernero, L. Inhibition of MptpB phosphatase from Mycobacterium tuberculosis impairs mycobacterial survival in macrophages. *J. Antimicrob. Chemother.* **2009**, *63*, 928–936.

(20) Weide, T.; Arve, L.; Prinz, H.; Waldmann, H.; Kessler, H. 3-Substituted indolizine-1-carbonitrile derivatives as phosphatase inhibitors. *Bioorg. Med. Chem. Lett.* **2006**, *16*, 59–63.

(21) Noren-Muller, A.; Reis-Correa, I.; Prinz, H.; Rosenbaum, C.; Saxena, K.; Schwalbe, H.; Vestweber, D.; Cagna, G.; Schunk, S.; Schwarz, O.; Schiewe, H.; Waldmann, H. Discovery of protein phosphatase inhibitor classes by biology-oriented synthesis. *Proc. Natl. Acad. Sci. U.S.A.* **2006**, *103*, 10606–10611.

(22) Reis-Correa, I.; Noren-Muller, A.; Ambrosi, H.; Jakupovic, S.; Saxena, K.; Schwalbe, H.; Kaiser, M.; Waldmann, H. Identification of inhibitors for mycobacterial protein tyrosine phosphatase B (MptpB) by biology-oriented synthesis (BIOS). *Chem. Asian J.* **2007**, *2*, 1109–1126.

(23) Noren-Muller, A.; Wilk, W.; Saxena, K.; Schwalbe, H.; Kaiser, M.; Waldmann, H. Discovery of a new class of inhibitors of Mycobacterium tuberculosis protein tyrosine phosphatase B by biology-oriented synthesis (BIOS). *Angew. Chem., Int. Ed.* **2008**, *47*, 5973–5977.

(24) Soellner, M. B.; Rawls, K. A.; Grundner, C.; Alber, T.; Ellman, J. A. Fragment-based substrate activity screening method for the identification of potent inhibitors of the *Mycobacterium* tuberculosis phosphatase PtpB. *J. Am. Chem. Soc.* **2007**, *129*, 9613–9615.

(25) Tan, L. P.; Wu, H.; Yang, P.-Y.; Kalesh, K.; Zhang, X.; Hu, M.; Srinivasan, R.; Yao, S. High-throughput discovery of *Mycobacterium* tuberculosis protein tyrosine phosphatase B (MptpB) inhibitors using click chemistry. *Org. Lett.* **2009**, *11*, 5102–5105.

(26) He, R.; Yu, Z.; He, Y.; Zeng, L.-F.; Xu, J.; Wu, L.; Gunawan, A. M.; Wang, L.; Jiang, Z.-X.; Zhang, Z.-Y. Double click reaction for the acquisition of a highly potent and selective mPTPB inhibitor. *ChemMedChem* **2010**, *5*, 2051−2056.
(27) Shen, G.; Wang, M.; Welch, T.; Blagg, B. Design, synthesis, and structure−activity relationships for chimeric inhibitors of Hsp90. *J. Org. Chem.* **2006**, *71*, 7618−7631.
(28) Tisdale, E. J.; Li, H.; Kim, S. H.; Theodorakis, E. A. Regioselective synthesis of the tricyclic core of lateriflorone. *Org. Lett.* **2003**, *5*, 1491−1494.
(29) Sonogashira, K.; Tohda, Y.; Hagihara, N. A convenient synthesis of acetylenes: catalytic substitutions of acetylenic hydrogen with bromoalkenes, iodoarenes and bromopyridines. *Tetrahedron Lett.* **1975**, *16*, 4467−4470.
(30) Chinchilla, R.; Nájera, C. The Sonogashira reaction: a booming methodology in synthetic organic chemistry. *Chem. Rev.* **2007**, *107*, 874−922.
(31) Yue, D.; Yao, T.; Larock, R. C. Synthesis of 2,3-disubstituted benzo[b]furans by the palladium-catalyzed coupling of o-iodoanisoles and terminal alkynes, followed by electrophilic cyclization. *J. Org. Chem.* **2005**, *70*, 10292−10296.
(32) Nathan, C. F.; Prendergast, T. J.; Wiebe, M. E.; Stanley, E. R.; Platzer, E.; Remold, H. G.; Welte, K.; Rubin, B. Y.; Murray, H. W. Activation of human macrophages: comparison of other cytokines with interferon-γ. *J. Exp. Med.* **1984**, *160*, 600−605.
(33) Yu, X.; Sun, J.-P.; He, Y.; Guo, X.-L.; Liu, S.; Zhou, B.; Hudmon, A.; Zhang, Z.-Y. Structure, inhibitor, and regulatory mechanism of Lyp, a lymphoid-specific tyrosine phosphatase implicated in autoimmune diseases. *Proc. Natl. Acad. Sci., U.S.A.* **2007**, *104*, 19767−19772.
(34) Zhang, X.; He, Y.; Liu, S.; Yu, Z.; Jiang, Z.-X.; Yang, Z.; Dong, Y.; Nabinger, S. C.; Wu, L.; Gunawan, A. M.; Wang, L.; Chan, R. J.; Zhang, Z.-Y. Salicylic acid-based small molecule inhibitor for the oncogenic Src homology-2 domain containing protein tyrosine phosphatase-2 (SHP2). *J. Med. Chem.* **2010**, *53*, 2482−2493.
(35) Mhaidat, N. M.; Wang, Y.; Kiejda, K. A.; Zhang, X. D.; Hersey, P. Docetaxel-induced apoptosis in melanoma cells is dependent on activation of caspase-2. *Mol. Cancer Ther.* **2007**, *6*, 752−761.